



# Nitrous oxide dynamics across nitrogen and pH gradients in headwater streams

Mette V. Carstensen<sup>1</sup>, Annelies J. Veraart<sup>2</sup>, Ida F. Peterse<sup>2,3</sup>, Nicole Wrage-Mönnig<sup>4</sup>, and Joachim Audet<sup>1</sup>

5

<sup>1</sup>Department of Ecosystems, Aarhus University, Aarhus, Denmark.

<sup>2</sup>Department of Ecology, Radboud Institute for Biological and Environmental Sciences, Radboud University, Nijmegen, the Netherlands

<sup>3</sup>Department of Microbiology, Radboud Institute for Biological and Environmental Sciences, Radboud University, Nijmegen, the Netherlands

<sup>4</sup>Grassland and Fodder Sciences, University of Rostock, Rostock, Germany

*Correspondence to:* Mette V. Carstensen ([mvc@ecos.au.dk](mailto:mvc@ecos.au.dk))

15

20

25



## Abstract

Headwater streams in agricultural landscapes can contribute substantially to nitrous oxide ( $\text{N}_2\text{O}$ ) emissions, yet the environmental controls on stream  $\text{N}_2\text{O}$  dynamics remain poorly resolved, particularly in systems with low pH. We investigated 72 Danish headwater streams spanning broad gradients in pH (5.0 - 8.8), land use, and soil type to identify the main drivers of  $\text{N}_2\text{O}$  variability. Nitrate ( $\text{NO}_3^-$ ) was the strongest predictor of  $\text{N}_2\text{O}$  saturation, and its positive association with  $\text{N}_2\text{O}$  intensified under acidic conditions according to linear mixed models. Ammonium, dissolved organic carbon, and stream depth also showed significant but weaker positive relationships with  $\text{N}_2\text{O}$ . Spatial differences among streams explained considerably more variation than seasonal or regional patterns, underscoring the dominance of local factors. Streams with  $\text{pH} < 6$  consistently exhibited higher  $\text{N}_2\text{O}$  saturation, and generalized additive modelling indicated a marked decline in  $\text{N}_2\text{O}$  levels beginning near pH 6. Despite generally high  $\text{N}_2\text{O}$  saturation, approximately 9 % of observations displayed undersaturation, which occurred mainly in streams with low  $\text{NO}_3^-$  concentrations and across all seasons. Our results indicate that acidic, weakly buffered catchments may enhance in-stream  $\text{N}_2\text{O}$  accumulation even at moderate nitrogen levels. These findings highlight the need to consider pH-related controls when assessing  $\text{N}_2\text{O}$  dynamics in freshwater networks and when designing mitigation strategies for agricultural landscapes.

## 40 1. Introduction

Nitrous oxide ( $\text{N}_2\text{O}$ ) is a potent greenhouse gas and ozone-depleting substance, with agriculture as its main anthropogenic source (Ravishankara et al., 2009; Ipcc, 2019). While terrestrial emissions are well studied, emissions from aquatic systems, especially, ditches, streams and rivers, remain less constrained (Maavara et al., 2019; Seitzinger and Kroese, 1998; Silverthorn et al., 2025). Recent evidence suggests riverine networks may contribute significantly to global  $\text{N}_2\text{O}$  budgets (Yao et al., 2020). In agricultural areas, a considerable share of applied nitrogen (N) fertilizers bypasses crop uptake and is transported into groundwater and surface waters, eventually reaching coastal waters. Along the hydrological continuum, dissolved N undergoes various biogeochemical transformations that can generate  $\text{N}_2\text{O}$ , either in soils and groundwater before entering streams, or directly within the stream channels.

Nitrous oxide is produced through a variety of biotic and abiotic transformations of N compounds in soils, sediments, and waters (Quick et al., 2019). Nitrification, the microbial oxidation of ammonia ( $\text{NH}_3$ ) or ammonium ( $\text{NH}_4^+$ ) to nitrate ( $\text{NO}_3^-$ ), can release  $\text{N}_2\text{O}$  as a by-product during its initial step (Butterbach-Bahl et al., 2013). In addition, nitrifier denitrification, a process carried out by ammonia-oxidizing bacteria under low-oxygen conditions, can also contribute to  $\text{N}_2\text{O}$  emissions (Wrage et al., 2001). Heterotrophic denitrification is the sequential reduction of  $\text{NO}_3^-$  to gaseous dinitrogen ( $\text{N}_2$ ), with  $\text{N}_2\text{O}$  formed as an intermediate step just before the final reduction to  $\text{N}_2$  (Knowles, 1982). Although nitrification and denitrification are typically regarded as the main pathways of  $\text{N}_2\text{O}$  production, abiotic processes, as well as their interaction, may also contribute substantially (Zhu-Barker et al., 2015; Grabb et al., 2017).



Soil acidification can strongly influence denitrification, particularly the terminal step in which  $\text{N}_2\text{O}$  is reduced to  $\text{N}_2$  (Šimek and Cooper, 2002; Firestone et al., 1980). This reduction is catalyzed by nitrous oxide reductase (*nosZ*), and under acidic conditions it is often impaired, resulting in elevated  $\text{N}_2\text{O}/(\text{N}_2 + \text{N}_2\text{O})$  ratios (Firestone et al., 1980). Although this effect  
60 is well documented in soils, the influence of low pH on  $\text{N}_2\text{O}$  levels in aquatic systems is less investigated (Audet et al., 2020) or limited to near-neutral pH (Clough et al., 2011; Baulch et al., 2012). To address this gap, we investigated the interplay between land use, hydromorphology, and stream water chemistry across a diverse set of Danish headwater streams. Denmark is particularly well suited for such an investigation because of its extensive acidic soils (podzols). Although these soils are generally less favorable for farming, they remain widely cultivated and heavily fertilized. This combination of naturally low  
65 pH and intensive agricultural practices creates conditions that are especially suitable for investigating the links between stream water acidity, nutrient inputs, and processes such as  $\text{N}_2\text{O}$  production. We hypothesize that streams with low pH exhibit disproportionately large  $\text{N}_2\text{O}$  saturation, particularly in agricultural catchments with large N inputs. In addition, we explore how different environmental factors beyond N and pH contribute to spatial and temporal variability in  $\text{N}_2\text{O}$  saturation, and which sources of variance, such as seasonal and temporal, are most influential.

## 70 2. Methods

### 2.1 Site and catchment characteristics

Sampling was conducted in 72 headwater streams located in Denmark, selected to obtain a wide range in pH, soil type, and land cover (Fig. 1+2). Many of these streams have been deepened and channelized, especially those located in agricultural landscapes. Due to regional geological variation, stream pH exhibits a pronounced east-west gradient (Thodsen et al., 2024).  
75 Eastern Denmark, including Zealand, Funen, and the easternmost part of Jutland, is underlain by calcareous glacial tills deposited during the Weichselian glaciation (Madsen, 1987). These sediments, originating from an ice advance from the Baltic Sea, are rich in chalk, which imparts a higher buffering capacity and contributes to elevated pH levels in surface waters (Fig. 1). In contrast, western Jylland is dominated by older, more leached glacial and meltwater deposits with lower carbonate content, resulting in reduced buffering capacity and generally lower stream pH. The catchments associated with each sampling  
80 location were delineated using a national digital elevation model (DEM) with a 10 m spatial resolution, obtained from the Danish Agency for Data Supply and Infrastructure. Delineation was carried out in ArcGIS Pro (version 3.5; ESRI Inc., Redlands, CA, USA) using the Fill, Flow Direction, and Watershed tools. Stream slope was quantified as the change in water-surface elevation over a 100 m reach, measured with a Leica GPS at the sampling site and a point 100 m upstream; where canopy impaired satellite reception, slope was derived from the DEM. Soil pH and soil type (JB number at 30–60 cm  
85 depth) for each catchment were extracted from Adhikari (2013). Land use within each catchment was quantified by calculating the percentage cover of major land use categories using data from the Danish Area Information System (Nielsen et al., 2000).

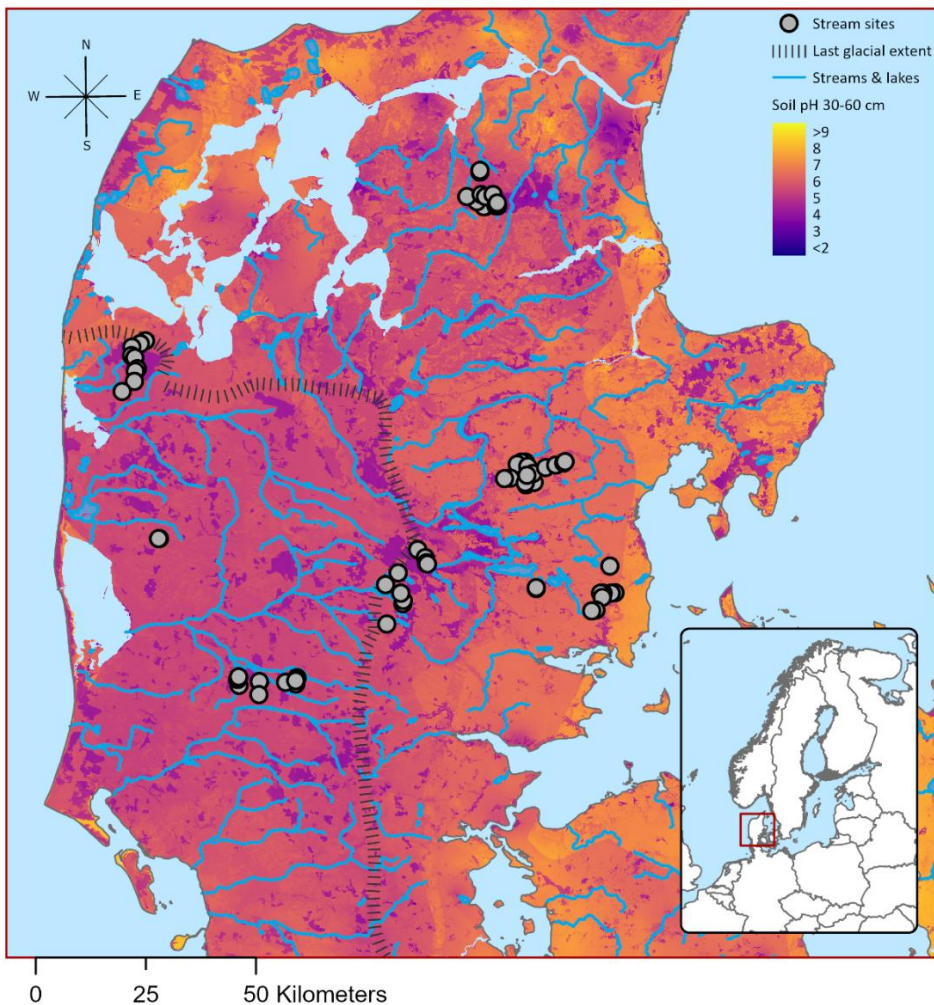


**Figure 1. Map of the 72 stream study sites, the pH of soil in a depth of 30-60 cm below surface, and the extent of the ice advance during the Weichselian glaciation (land area south-west of this line was ice free).**



**Figure 2. Photographs of Danish headwater streams with stream identity.**

## 2.2 Sampling

95 Water samples were taken from all streams seasonally during summer (19–26 August 2022), autumn (3–14 November 2022),  
winter (17–30 January 2023), and spring (19 April – 4 May 2023) (Fig. 2). Of these, ten streams (Stream 1–10) were sampled  
monthly from April 2022 to April 2023. During the summer sampling campaign, 12 of the 72 streams were dry, with three  
remaining dry until the winter sampling period. Water samples were collected 20–30 cm from the stream bank using a 250 mL  
polypropylene bottle and stored in a transportable cooler. At each site, stream water velocity, width, and depth were measured.

100 Stream water velocity and depth were measured across the stream with three points (right, middle and left). Stream velocity  
was measured using a vane wheel anemometer (Höntzsch GmbH & Co. KG, Germany). The discharge was calculated from



average stream dimensions and average velocity. Vegetation cover was visually estimated and recorded as a percentage, while the presence of iron ochre deposits was assessed on a scale from 0 to 3 (low to high abundance). Stream water temperature, dissolved oxygen, electrical conductivity, and pH were measured in situ using a multi-parameter probe (YSI Professional Plus, 105 Xylem Analytics, USA). Samples for dissolved N<sub>2</sub>O analysis were collected by drawing 50 mL of stream water into a syringe, followed by the addition of 10 mL of ambient air. The syringe was sealed using a stopcock and shaken vigorously for 1 minute by holding the piston, while keeping the syringe in the shade to minimize changes in temperature. The headspace gas was then transferred into a 5.9 mL pre-evacuated glass vial. Samples were stored in the dark until analysis. In addition, a 5.9 mL ambient air sample was collected above the water surface at each sampling location. Data on precipitation and atmospheric pressure 110 were obtained from the Danish meteorological institute.

### 2.3 Water chemistry

The samples for analysis of dissolved organic carbon (DOC), NO<sub>3</sub><sup>-</sup>, NH<sub>4</sub><sup>+</sup>, and soluble reactive phosphorus (SRP) were filtered within 24 hours in the laboratory using Whatman GF/C filters (pore size 0.45 µm), which were rinsed with 300 ml demineralized water before use. Both filtered and unfiltered samples were stored cold (3–5 °C) and dark until analysis. The 115 samples for NO<sub>3</sub><sup>-</sup> and sulphate (SO<sub>4</sub><sup>2-</sup>) determination were analysed according to Danish standard Ds/En Iso 10304 (2009) by ion chromatography (Dionex ICS-1500 IC-system) with an anion Micro Membrane Suppressor (AMMS III 4 mm) as basic eluent. The system was equipped with a guard column (IonPac AG22) and a separator column (IonPac AS22). The eluent was a mixture of 4.5 mM Na<sub>2</sub>CO<sub>3</sub> and 1.4 mM NaHCO<sub>3</sub>. All samples for ion chromatography were filtered through a double-layered 0.22 µm glass fibre filter (SNY2225, Frisenette ApS, Knebel, Denmark). Ammonium (NH<sub>4</sub><sup>+</sup>-N), total P (TP) and SRP 120 were measured colorimetrically on a spectrophotometer (Shimadzu 1700, Shimadzu Corp., Kyoto, Japan) according to the Danish/European standard methods Ds/En Iso 11732 (2005) for NH<sub>4</sub><sup>+</sup> and Ds/En Iso 6878 (2004) for TP and SRP. Total organic carbon, DOC and TN were both measured on a TOC-L analyser equipped with a TNM-L module (Shimadzu, Kyoto, Japan) at a temperature of 720 °C following Ds/En Iso 1484 (1997) and Ds/En 12260 (2003), respectively.

### 2.4 Dissolved nitrous oxide analysis

125 The headspace concentrations of N<sub>2</sub>O were determined using a dual-inlet Agilent 7890 GC system interfaced with a CTC CombiPal autosampler (Agilent, Denmark) configured and calibrated with standard gases according to Petersen et al. (2012), with detection limits of 0.15 ppm for N<sub>2</sub>O. The aqueous concentrations of N<sub>2</sub>O were calculated from the headspace gas concentrations according to Henry's law and using Henry's constant corrected for water temperature and atmospheric pressure at the sampling time (Weiss and Price, 1980). Stream water was considered undersaturated with respect to N<sub>2</sub>O when dissolved 130 concentrations were lower than the theoretical equilibrium concentration calculated from Henry's law the global annual mean atmospheric concentration of 0.336 ppm. The saturation levels were classified as undersaturated (<95 %), ~atmospheric equilibrium (95 %–105 %), and oversaturated (>105 %) following Aho et al. (2023).



## 2.5 Sediment analysis

135 Dry matter content was determined following Ds/En 15934 (2012) and the loss on ignition, following Ds/En 15934 (2012).  
For more details see appendix.

## 2.6 Data analysis and statistical analysis

All statistical analyses were performed using R version 4.4.3(R Core Team, 2025). The N<sub>2</sub>O saturation was log transformed to ensure normality. Linear mixed-effects models (LMM) were used to identify environmental drivers of N<sub>2</sub>O saturation using  
140 the lmer() function from the lmer4 R package (Bates et al., 2015). To account for the hierarchical data structure and repeated measurements within the same stream, we included a random intercept for stream identity. Prior to model development the correlation between predictor variables were checked, to ensure that parameters with a correlation coefficient above 0.5 were not included (Fig. A1). In addition, we calculated the variance inflation factor (VIF) to further evaluate potential collinearity among predictors (Table A1). All continuous predictor variables were standardized (z-transformed: centered and scaled to unit  
145 variance) to ensure comparability of effect estimates and facilitate interpretation of interaction terms. Model selection followed a backward elimination procedure, where non-significant predictors were sequentially removed. Model assumptions were evaluated through residual diagnostics, including visual inspection of Q-Q plots and residual vs. fitted plots (Zuur et al., 2009). Linear mixed-effects models were also applied to assess temporal and spatial differences in N<sub>2</sub>O saturation, while accounting for repeated measures within streams. Pairwise comparisons between regions and seasons were conducted using estimated  
150 marginal means via the emmeans R package (Lenth, 2025). P-values were adjusted for multiple testing using the Bonferroni method to control the family-wise error rate (Haynes, 2013). The relationship between log-transformed N<sub>2</sub>O saturation and stream pH was modeled using a generalized additive model (GAM) with a smooth pH term fitted by REML. Derivatives of the smooth were used to identify pH ranges where N<sub>2</sub>O changed significantly with pH. The first pH at which the derivative became significantly negative was defined as the onset of decline, and the pH with the most negative derivative as the point of  
155 steepest decline. Robustness of the onset threshold was evaluated using bootstrap resampling (n = 500).

## 3 Results

### 3.1 Spatiotemporal variation

During the study period (April 2022 to March 2023) the mean ( $\pm$  SD) precipitation was  $741 \pm 102$  mm and mean air temperature was  $8.9 \pm 0.4$  °C (Table 1). Mean N<sub>2</sub>O concentration between all sampling sites were  $2.4 \pm 2.8$  µg N L<sup>-1</sup> ranging from 0.1 to 22.2  
160 µg N L<sup>-1</sup>. In the ten streams monitored monthly, N<sub>2</sub>O saturation showed substantial variability both temporally and across individual streams. The stream with the lowest water pH (Stream 6, mean pH=5.8±0.2) generally exhibited higher N<sub>2</sub>O saturation (Fig. 3, Fig. A2). For most streams N<sub>2</sub>O saturation peaked during late winter and early spring coinciding with



elevated  $\text{NO}_3^-$  concentrations (Fig. 3, Fig. A3). In contrast,  $\text{NH}_4^+$  levels remained low and relatively stable throughout the study period (Fig. A4). Consistent with patterns observed for streams with monthly monitoring, mean  $\text{N}_2\text{O}$  saturation across all 165 streams were significantly higher during winter, compared to summer  $\text{N}_2\text{O}$  saturation (Table A2+A3). Summer  $\text{N}_2\text{O}$  saturation was also significantly lower compared to spring and autumn (Table A3). Stream-level differences explained the largest share of variance, with an intra-class correlation coefficient (ICC) of 0.67 according to our LLM (between-stream variance = 0.119; residual = 0.059). The remaining 33 % of the variance was attributable to within-stream variability. Regional variation accounted for a smaller proportion (ICC = 0.15; variance = 0.030; residual = 0.173), while seasonal differences were negligible 170 (ICC = 0.016; variance = 0.0032; residual = 0.195).

**Table 1.** Mean, SD, min and max of key parameters for Danish headwater streams, where  $\text{N}_2\text{O}$  =nitrous oxide,  $\text{NO}_3^-$  =nitrate, TN=total nitrogen,  $\text{NH}_4^+$ =ammonium, TOC =total organic carbon, DOC =dissolved organic carbon, TP=total phosphorus, SRP =soluble reactive phosphorus,  $\text{SO}_4^{2-}$ =sulphate, and  $\text{O}_2$ = dissolved oxygen.

	Mean	SD	Min	Max	175
<b>Temperature (water)</b>	9.3	3.6	-0.2	19.5	
<b>Flow velocity (m s<sup>-1</sup>)</b>	0.24	0.22	0.005	1.49	
<b><math>\text{N}_2\text{O}</math> (µg N L<sup>-1</sup>)</b>	2.4	2.8	0.1	22.2	
<b><math>\text{N}_2\text{O}</math> (sat, %)</b>	608	722	27	5991	
<b><math>\text{CO}_2</math> (µg C L<sup>-1</sup>)</b>	2282	1981	69	12981	
<b>TN (mg L<sup>-1</sup>)</b>	3.3	2.8	0.02	14.9	180
<b><math>\text{NO}_3^-</math> (mg N L<sup>-1</sup>)</b>	2.6	2.6	0.02	13.7	
<b><math>\text{NH}_4^+</math> (mg N L<sup>-1</sup>)</b>	0.08	0.30	0.0001	4.42	
<b>TOC (mg L<sup>-1</sup>)</b>	10.3	9.9	0.7	60.4	
<b>DOC (mg L<sup>-1</sup>)</b>	9.2	9.3	1.1	54.3	
<b>TP (mg L<sup>-1</sup>)</b>	0.27	1.54	0.01	28.63	
<b>SRP (mg L<sup>-1</sup>)</b>	0.04	0.07	0.001	0.94	185
<b><math>\text{SO}_4^{2-}</math> (mg L<sup>-1</sup>)</b>	40	161	2	2810	
<b><math>\text{O}_2</math> (mg L<sup>-1</sup>)</b>	9.6	2.7	0.5	18.7	
<b>pH</b>	7.1	0.7	5.0	8.8	
<b>Stream depth (cm)</b>	20.6	13.7	0.2	68.3	
<b>Stream width (cm)</b>	149	84	25	660	
<b>Stream slope (%)</b>	7.0	9.5	0.0	68.5	190
<b>Intensive agriculture (%)</b>	48	31	0	94	
<b>Forest (%)</b>	26	27	0	88	

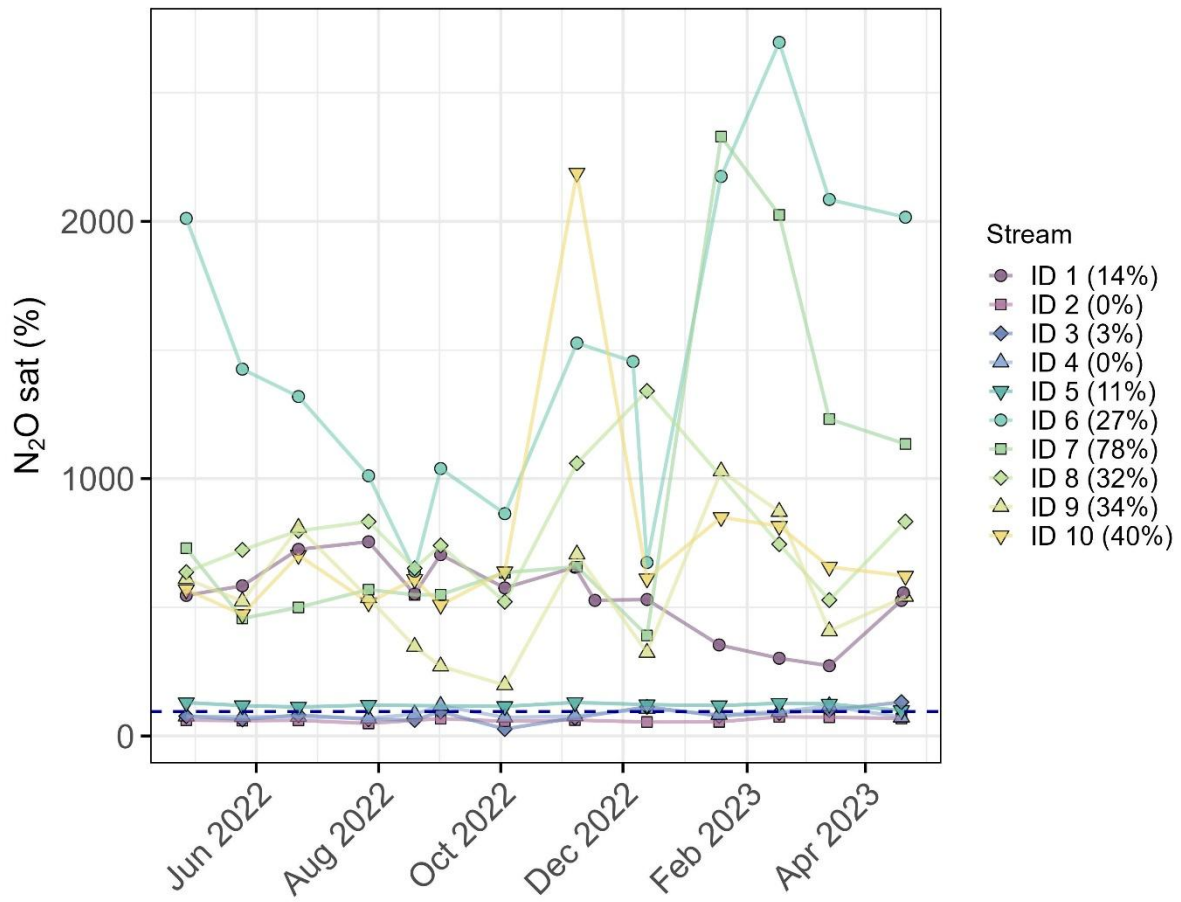


Figure 3. Nitrous oxide (N<sub>2</sub>O) saturation (%) in stream water from ten streams (ID 1–10) monitored monthly. Stream-specific percentages of intensive agriculture within the catchment are given in the legend. The dark blue dashed line indicates the threshold below which N<sub>2</sub>O concentrations are considered undersaturated relative to atmospheric equilibrium.

### 3.3 Drivers of nitrous oxide dynamics

The final model retained NO<sub>3</sub><sup>−</sup>, pH, NH<sub>4</sub><sup>+</sup>, DOC, land use, and stream depth as significant fixed effects (Table 2, Fig. A5). All retained predictors were positively correlated with N<sub>2</sub>O concentrations, except pH. A significant negative interaction with pH (Estimate = −0.10,  $p < 0.001$ ) was included, indicating that N<sub>2</sub>O increased with NO<sub>3</sub><sup>−</sup> and the effect of NO<sub>3</sub><sup>−</sup> was amplified under acidic conditions (Table 2). The model captured notable variation between stream locations (random intercept variance

= 0.041±0.020), although a considerable amount of unexplained variation remained (residual variance = 0.041±0.020) (Fig. A6). Fixed effects alone explained approximately 47 % of the variation in N<sub>2</sub>O (marginal R<sup>2</sup>), while the full model (including stream-level random effects) accounted for about 73 % (conditional R<sup>2</sup>) (Table A4). Initially SRP appeared as a significant predictor of N<sub>2</sub>O saturation, but this relationship was driven by a single high observation and became non-significant upon its exclusion. CO<sub>2</sub> was excluded due to a strong correlation with pH which might have introduced multicollinearity into the statistical model. Variables such as water temperature, oxygen in stream water, precipitation, sulphate and flow velocity were excluded from the final model due to a lack of statistical significance.

210 215 **Table 2. Results from linear mixed-effects model analysis with individual streams as random effects with pH, nitrate (NO<sub>3</sub><sup>-</sup>), dissolved organic carbon (DOC), ammonium (NH<sub>4</sub><sup>+</sup>), stream depth and interaction between pH and NO<sub>3</sub><sup>-</sup>. All continuous predictor variables were standardized (z-transformed: centered and scaled to unit variance).**

	Estimate	SE	DF	t value	p value
<b>(Intercept)</b>	2.587	0.027	69	93.9	< 0.05
NO <sub>3</sub> <sup>-</sup>	0.226	0.021	300	10.7	< 0.001
<b>pH</b>	-0.181	0.022	231	-8.03	< 0.001
NH <sub>4</sub> <sup>+</sup>	0.036	0.011	310	3.10	< 0.01
<b>DOC</b>	0.048	0.014	362	3.38	< 0.001
<b>Stream depth</b>	0.069	0.016	361	4.37	< 0.001
<b>pH: NO<sub>3</sub><sup>-</sup></b>	-0.107	0.021	363	-5.06	< 0.001

### 3.4 The effect of pH

220 225 The N<sub>2</sub>O saturation increased with NO<sub>3</sub><sup>-</sup> concentrations, but the magnitude of this response varied markedly with pH (Fig. 4). The highest N<sub>2</sub>O saturations were observed at low pH, particularly below pH 6, where several observations exceeded 2,000 % saturation even at moderate NO<sub>3</sub><sup>-</sup> levels. Derivative analysis of the GAM indicated that N<sub>2</sub>O saturation began to decline at pH ≈ 5.95, with the steepest decrease occurring at pH ≈ 6.37, defining a transition zone over which N<sub>2</sub>O saturation dropped most sharply (Fig. A7). Bootstrap resampling confirmed the robustness of the start-of-decline estimate, with a median of 5.96 and a 95 % confidence interval of 5.83–6.19. The N<sub>2</sub>O saturation was significantly higher for streams with pH < 6 (mean: 1275±927 µg L<sup>-1</sup>) compared to streams with pH > 6 (mean: 485±576 µg L<sup>-1</sup>) according to LLM analysis taking stream identity into account ( $\beta = 0.4 \pm 0.1$ ,  $p < 0.001$ ).

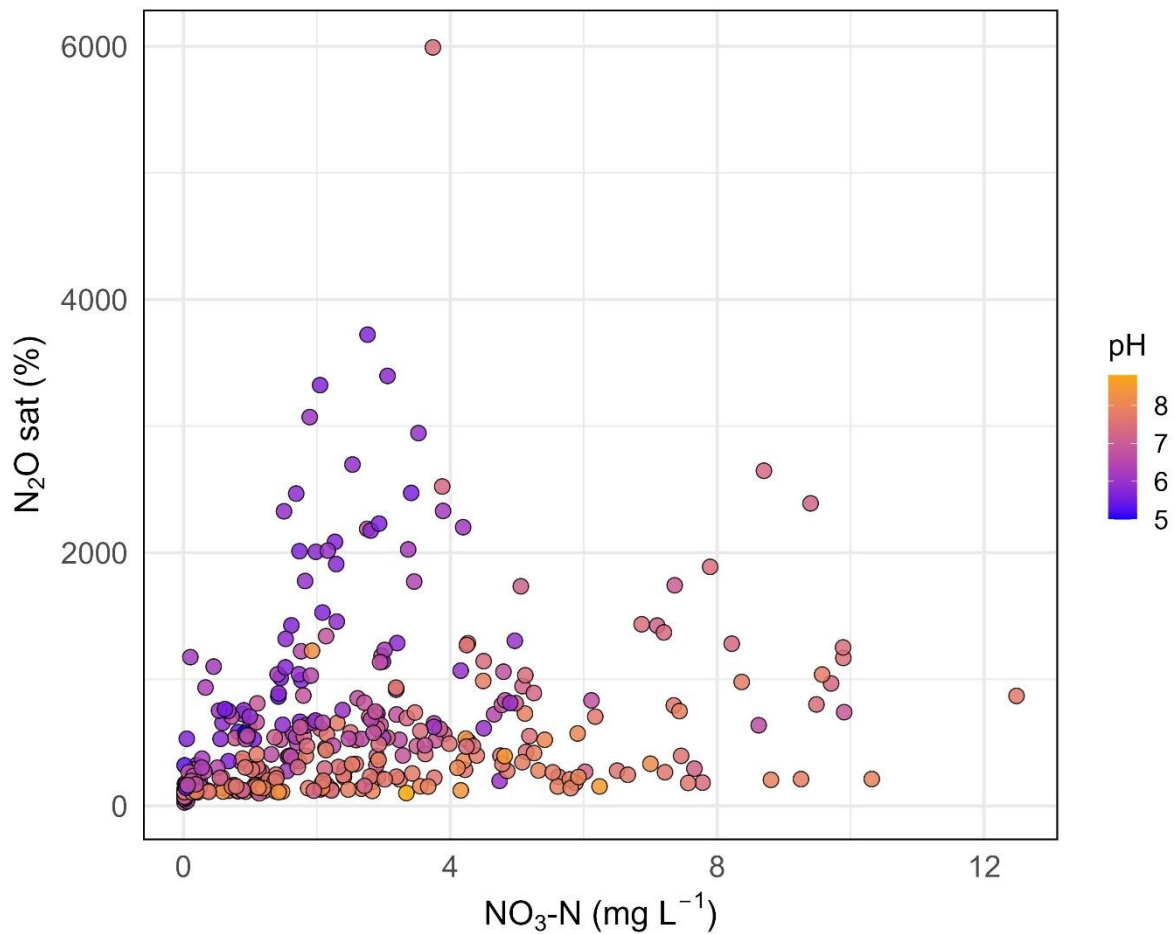


Figure 4. Nitrous oxide ( $\text{N}_2\text{O}$ ) saturation versus nitrate ( $\text{NO}_3^-$ -N) concentration. The color gradient indicates the pH in the stream water.

230

### 3.5 Streams as net nitrous oxide sinks

Streams acted as net  $\text{N}_2\text{O}$  sinks in approximately 9 % of observations, as indicated by water column undersaturation relative to atmospheric equilibrium. Mean  $\text{N}_2\text{O}$  undersaturation was 69 % ranging from 27 to 94 %. Nitrous oxide undersaturation was observed primarily in streams with low  $\text{NO}_3^-$  concentrations, and there was no seasonal tendency. Prolonged periods of 235 undersaturation were observed in three semi-natural streams. One stream (Stream 2) was undersaturated during all sampling campaigns, whereas Streams 3 and 4 were undersaturated in approximately 75 % of the campaigns. In addition, a single occurrence of undersaturation was observed in a stream receiving water from an agriculturally dominated catchment (stream 25).



## 4 Discussion

### 240 4.1 In-stream nitrous oxide dynamics and variation

Our observed  $\text{N}_2\text{O}$  concentrations (mean  $2.4 \pm 2.8 \mu\text{g N L}^{-1}$  or  $608 \pm 722 \%$ ) were somewhat higher than levels from past studies of stream and rivers: median  $1.0 \mu\text{g N L}^{-1}$  in Sweden (Audet et al., 2020), mean  $0.8 \mu\text{g N L}^{-1}$  or  $236 \%$  in Michigan in United States (Beaulieu et al., 2008),  $114 \pm 20 \%$  in New Zealand (Clough et al., 2011) and  $184 \pm 1,081 \%$  in United States (Aho et al., 2023). Stream water  $\text{N}_2\text{O}$  concentrations are the result of complex interactions among potential transport pathways (e.g. in-stream production, external input), within-stream physical factors (e.g. turbulence, slope) and biogeochemical conditions (e.g. pH, redox conditions). Here, we nonetheless assessed whether statistically robust relationships exist between  $\text{N}_2\text{O}$  saturation and selected in-stream environmental variables associated with  $\text{N}_2\text{O}$  production and consumption. Our finding that  $\text{NO}_3^-$  was a significant predictor of  $\text{N}_2\text{O}$  saturation is consistent with earlier studies (Baulch et al., 2012; Clough et al., 2011; Beaulieu et al., 2009). These findings may imply that heterotrophic denitrification contributes substantially to  $\text{N}_2\text{O}$  dynamics, whether 245 through enhanced process rates or altered product ratios under elevated  $\text{NO}_3^-$  levels, though further evidence is needed to confirm this. Metagenomic analysis of the sediment from two agricultural streams from our stream network (Peterse et al., in prep.) confirmed the presence of denitrification genes (*nirS*, *norB*, *nosZ*). Our results further indicate that the effect of  $\text{NO}_3^-$  on  $\text{N}_2\text{O}$  levels is stronger under acidic conditions. This implies that low pH in streams may promote elevated  $\text{N}_2\text{O}$  concentrations even under low N availability, consistent with Audet et al. (2020), who observed similar  $\text{N}_2\text{O}$  concentrations in 250 forested ( $\text{pH} < 6$ ) and agricultural streams despite much higher N concentrations in the latter.

Hydrological characteristics such as water residence time, slope, stream depth, flow velocity, and physical structure also influence  $\text{N}_2\text{O}$  concentration by affecting biogeochemical processes and gas exchange (Marzadri et al., 2021; Tonina et al., 2021; Mulholland et al., 2008; Mwanake et al., 2023). Our results show that deeper streams tend to exhibit higher  $\text{N}_2\text{O}$  saturation (Fig. A7). This pattern may be partially explained by the negative association between stream depth and lower pH 260 levels. Physical constraints on gas exchange may also contribute, as deeper water bodies typically have lower surface area-to-volume ratios, potentially limiting the evasion of  $\text{N}_2\text{O}$  to the atmosphere, leading to higher  $\text{N}_2\text{O}$  concentrations in the water column. Several potentially important controls on  $\text{N}_2\text{O}$  concentrations were not accounted for in our study design, particularly those related to hydrological flow paths. Groundwater, often oversaturated with  $\text{N}_2\text{O}$  (Jurado et al., 2017; Von Der Heide et al., 2008), can significantly influence stream concentrations, particularly in headwater systems where it constitutes a major 265 portion of baseflow (Bisson et al., 2025). Drain systems can deliver concentrated pulses of  $\text{NO}_3^-$  and  $\text{N}_2\text{O}$  directly into streams. Reay et al. (2003) reported  $\text{N}_2\text{O}$  concentrations at drain outlets up to five times higher than those measured 100 meters downstream, suggesting rapid degassing upon discharge. Our study showed that seasonal patterns were weak, with slightly lower  $\text{N}_2\text{O}$  saturation in summer. This may reflect reduced substrate availability, enhanced N assimilation, and/or increased denitrification to  $\text{N}_2$  under warmer conditions. Overall, our findings align with previous studies reporting inconsistent 270 seasonality a (Audet et al., 2020; Beaulieu et al., 2008; Hama-Aziz et al., 2017; Aho et al., 2022; Cole and Caraco, 2001; Rosamond et al., 2012), reinforcing the importance of local over temporal drivers.



## 4.2 The direct effect of pH

In our study,  $\text{N}_2\text{O}$  saturation was negatively correlated with pH, and this effect was most pronounced at pH values below 6. Whether this relationship reflects a direct influence of pH or an indirect one mediated by other environmental variables remains

275 unresolved, and it will most likely depend on the dominant  $\text{N}_2\text{O}$  production pathway. Only a small number of studies have investigated  $\text{N}_2\text{O}$  concentrations in streams with low pH (Audet et al., 2020). In contrast, the effect of pH on  $\text{N}_2\text{O}$  is well documented in soils, where numerous studies have demonstrated that low pH can impair  $\text{N}_2\text{O}$  reduction and shift end-product ratios toward  $\text{N}_2\text{O}$  rather than  $\text{N}_2$  (Šimek and Cooper, 2002; Firestone et al., 1980; Liu et al., 2014; Qiu et al., 2024). This impairment is linked to reduced functionality of *nosZ*, the enzyme responsible for reducing  $\text{N}_2\text{O}$  to  $\text{N}_2$  (Firestone et al., 1980).

280 Metagenomic data from the sediment from two of our study streams (Peterse et al., in prep.) revealed that *nosZ* was only slightly less abundant in an acidic stream compared with a neutral stream. However, previous studies have demonstrated that gene presence alone is a poor indicator of  $\text{N}_2\text{O}$  reduction capacity under low pH conditions, as acidic environments primarily impair *nosZ* enzyme functionality rather than gene abundance (Liu et al., 2014; Olaya-Abril et al., 2021). The limited number of studies in streams means that the generality of the pH– $\text{N}_2\text{O}$  relationship across diverse landscapes is still poorly understood.

285 One reason this effect has not been widely reported previously may be that earlier studies examined streams with relatively narrow and high pH ranges such as 7.2–9.0 (Clough et al., 2011), or 7.55–8.43 (Baulch et al., 2012). In other cases, pH was measured, but results were not shown (Beaulieu et al., 2009; Hinshaw and Dahlgren, 2013) or pH was not measured (Baulch et al., 2011a; Stow et al., 2005). More research is needed to determine whether similar pH– $\text{N}_2\text{O}$  interactions operate under different climatic, hydrological, and biogeochemical conditions.

## 290 4.3 Indirect effects of pH

A range of environmental conditions and interactions influenced by pH may shift N transformation pathways toward processes that yield higher  $\text{N}_2\text{O}$  production. Under acidic conditions, nitrification intermediates such as hydroxylamine ( $\text{NH}_2\text{OH}$ ) and nitric oxide ( $\text{NO}$ ) can undergo chemical conversion to  $\text{N}_2\text{O}$  via non-enzymatic pathways (Zhu-Barker et al., 2015). A significant, but weak, positive correlation between  $\text{NH}_4^+$  and  $\text{N}_2\text{O}$  indicate that nitrification, nitrifier denitrification, coupled

295 nitrification-denitrification or nitrification coupled to abiotic processes may also contribute to  $\text{N}_2\text{O}$  production. The  $\text{NH}_4^+$  concentrations in streams were generally low, but it is possible that  $\text{NH}_4^+$  was released through the mineralization of organic matter in sediments, providing a substrate for nitrification (Arango and Tank, 2008). Supporting this, sediment data from ten streams with monthly monitoring showed that  $\text{NH}_4^+$  concentrations were consistently higher in sediments than in the overlying water (Peterse et al., in prep.). Microbial community profiling via 16S rRNA gene sequencing revealed nitrifiers in ten streams,

300 with acidophilic Nitrosotaleaceae dominating acidic sites, indicating that pH might alter community structure (Peterse et al., in prep.). Another potential  $\text{N}_2\text{O}$  source is chemodenitrification (Wankel et al., 2017), where oxidized N species are reduced by  $\text{Fe}^{2+}$ , which may be important in iron-rich, acidic soils such as western Jutland, but its contribution could not be confirmed because  $\text{Fe}^{2+}$  and abiotic processes were not measured directly.



#### 4.4 Nitrous oxide undersaturation

305 Freshwater ecosystems have been recognized as potential sinks for N<sub>2</sub>O for some time (Kroeze et al., 2007), yet this role remains largely ignored in both global and national greenhouse gas inventories (Aho et al., 2023; Webb et al., 2019). Kroeze et al. (2007) proposed that inland waters can function as net N<sub>2</sub>O sinks when N<sub>2</sub>O consumption processes exceed in situ production and atmospheric invasion. In our study undersaturated was observed for three streams located in areas with low impact from agriculture, and thus low stream water N concentrations. This finding is consistent with previous studies  
310 demonstrating that low N availability is a key factor influencing N<sub>2</sub>O undersaturation in streams (Kroeze et al., 2007; Baulch et al., 2011b; Aho et al., 2023). Samples collected from streams across the United States, as part of the National Ecological Observatory Network, showed that 30 % of the samples (678 of 2,288) were undersaturated. In our study undersaturation was observed across all seasons, with no statistically significant seasonal variation, implying that temporal factors such as temperature or hydrological conditions may play a lesser role than N status. Besides NO<sub>3</sub><sup>-</sup>, N<sub>2</sub>O undersaturation has also been  
315 linked to low oxygen and high DOC, (Baulch et al., 2011b; Borges et al., 2019).

### 5. Conclusions

Our study indicates that streams draining acidic catchments with low buffering capacity can exhibit elevated N<sub>2</sub>O saturation even when NO<sub>3</sub><sup>-</sup> concentrations are only moderate. Consequently, landscapes with acidic soils and limited buffering capacity could contribute more to regional N<sub>2</sub>O emissions than currently assumed in large-scale inventories, although the mechanisms  
320 behind the pH sensitivity require further investigation. Globally, acidic soils cover nearly one-third of the ice-free land surface (Soil Atlas of Europe, 2005), and in many regions, they coincide with areas of intensive agriculture (Guo et al., 2010). Implementing management strategies that reduce N inputs or surpluses in such systems could help mitigate in-stream N<sub>2</sub>O formation. However, more research is needed to determine whether similar patterns occur in other regions of the world, particularly in tropical and subtropical landscapes. Despite generally high N<sub>2</sub>O saturation, a small fraction of the observed  
325 streams showed undersaturation, occurring mainly in low-NO<sub>3</sub><sup>-</sup> streams with no seasonal variation, demonstrating that headwater streams can function as both sources and sinks of N<sub>2</sub>O.

### Acknowledgement

We thank Anne Hasselholt Andersen, Ditte Christensen, Emil Skole and the technical staff at Aarhus University for their help in the collection and analysis of samples. This study received support from the Independent Research Fund Denmark project  
330 DrivNOS grant nr. 0217-00021B.



## Author contribution

JA conceived the original idea, JA and MC planned the field campaigns; MC and IP performed the measurements; MC analyzed the data; MC wrote the manuscript draft; JA, AV, IP and NW reviewed and edited the manuscript. JA, NW, and AV supervised the project.

## 335 Data availability statement

All data used in this study are available from Zenodo at <https://zenodo.org/records/18457449>.

## Competing interests

The authors declare that they have no competing interests.

## References

340 Adhikari, K.: Soil mapping in Denmark using digital soil mapping Techniques, 2013.

Aho, K. S., Maavara, T., Cawley, K. M., and Raymond, P. A.: Inland Waters can Act as Nitrous Oxide Sinks: Observation and Modeling Reveal that Nitrous Oxide Undersaturation May Partially Offset Emissions, *Geophysical Research Letters*, 50, e2023GL104987, <https://doi.org/10.1029/2023GL104987>, 2023.

Aho, K. S., Fair, J. H., Hosen, J. D., Kyzivat, E. D., Logozzo, L. A., Weber, L. C., Yoon, B., Zarnetske, J. P., and Raymond, 345 P. A.: An intense precipitation event causes a temperate forested drainage network to shift from N<sub>2</sub>O source to sink, *Limnology and Oceanography*, 67, S242-S257, <https://doi.org/10.1002/lno.12006>, 2022.

Arango, C. P. and Tank, J. L.: Land use influences the spatiotemporal controls on nitrification and denitrification in headwater streams, *Journal of the North American Benthological Society*, 27, 90-107, 10.1899/07-024.1, 2008.

Audet, J., Bastviken, D., Bundschuh, M., Buffam, I., Feckler, A., Klemedtsson, L., Laudon, H., Löfgren, S., Natchimuthu, S., 350 Öquist, M., Peacock, M., and Wallin, M. B.: Forest streams are important sources for nitrous oxide emissions, *Global Change Biology*, 26, 629-641, <https://doi.org/10.1111/gcb.14812>, 2020.

Bates, D., Mächler, M., Bolker, B., and Walker, S.: Fitting Linear Mixed-Effects Models Using lme4, *Journal of Statistical Software*, 67, 1 - 48, 10.18637/jss.v067.i01, 2015.

Baulch, H., Dillon, P., Maranger, R., Venkiteswaran, J., Wilson, H., and Schiff, S.: Night and Day: Short-Term Variation in 355 Nitrogen Chemistry and Nitrous Oxide Emissions from Streams, *Freshwater Biology*, 57, 10.1111/j.1365-2427.2011.02720.x, 2012.

Baulch, H. M., Schiff, S. L., Maranger, R., and Dillon, P. J.: Nitrogen enrichment and the emission of nitrous oxide from streams, *Global Biogeochemical Cycles*, 25, <https://doi.org/10.1029/2011GB004047>, 2011a.



Baulch, H. M., Schiff, S. L., Thuss, S. J., and Dillon, P. J.: Isotopic Character of Nitrous Oxide Emitted from Streams,  
360 Environmental Science & Technology, 45, 4682-4688, 10.1021/es104116a, 2011b.

Beaulieu, J. J., Arango, C. P., and Tank, J. L.: The Effects of Season and Agriculture on Nitrous Oxide Production in Headwater  
Streams, Journal of Environmental Quality, 38, 637-646, <https://doi.org/10.2134/jeq2008.0003>, 2009.

Beaulieu, J. J., Arango, C. P., Hamilton, S. K., and Tank, J. L.: The production and emission of nitrous oxide from headwater  
streams in the Midwestern United States, Global Change Biology, 14, 878-894, <https://doi.org/10.1111/j.1365-2486.2007.01485.x>, 2008.

365 Bisson, A. M., Liu, F., Moore, E. M., Briggs, M. A., and Helton, A. M.: Preferential Groundwater Discharges Along Stream  
Corridors Are Disregarded Sources of Greenhouse Gases, Journal of Geophysical Research: Biogeosciences, 130,  
e2024JG008395, <https://doi.org/10.1029/2024JG008395>, 2025.

Borges, A. V., Darchambeau, F., Lambert, T., Morana, C., Allen, G. H., Tambwe, E., Toengaho Sembaito, A., Mambo, T.,  
370 Nlandu Wabakhangazi, J., Descy, J. P., Teodoru, C. R., and Bouillon, S.: Variations in dissolved greenhouse gases (CO<sub>2</sub>,  
CH<sub>4</sub>, N<sub>2</sub>O) in the Congo River network overwhelmingly driven by fluvial-wetland connectivity, Biogeosciences, 16, 3801-  
3834, 10.5194/bg-16-3801-2019, 2019.

Butterbach-Bahl, K., Baggs, E. M., Dannenmann, M., Kiese, R., and Zechmeister-Boltenstern, S.: Nitrous oxide emissions  
from soils: how well do we understand the processes and their controls?, Philosophical Transactions of the Royal Society B:  
375 Biological Sciences, 368, 20130122, doi:10.1098/rstb.2013.0122, 2013.

Clough, T. J., Buckthought, L. E., Casciotti, K. L., Kelliher, F. M., and Jones, P. K.: Nitrous Oxide Dynamics in a Braided  
River System, New Zealand, Journal of Environmental Quality, 40, 1532-1541, <https://doi.org/10.2134/jeq2010.0527>, 2011.

Cole, J. J. and Caraco, N. F.: Emissions of nitrous oxide (N<sub>2</sub>O) from a tidal, freshwater river, the Hudson River, New York,  
Environ Sci Technol, 35, 991-996, 10.1021/es0015848, 2001.

380 DS/EN 12260: Water Quality - Determination of Nitrogen- Determination of Bound Nitrogen (TNB), Following Oxidation to  
Nitrogen Oxides, 2003.

DS/EN 15934: Sludge, treated biowaste, soil and waste – Calculation of dry matter fraction after determination of dry residue  
or water content, 2012.

DS/EN ISO 1484: Water Analysis - Guidelines for the Determination of Total Organic Carbon (TOC) and Dissolved Organic  
385 Carbon (DOC), 1997.

DS/EN ISO 6878: Water quality - Determination of phosphorus - Ammonium molybdate spectrometric method, 2004.

DS/EN ISO 10304: Water Quality – Determination of Dissolved Anions by Liquid Chromatography of Ions – Part 1:  
Determination of Bromide, Chloride, Fluoride, Nitrate, Nitrite, Phosphate and Sulfate, 2009.

DS/EN ISO 11732: Water Quality - Determination of Ammonium Nitrogen - Method by Flow Analysis (CFA and FIA) and  
390 Spectrometric Detection, 2005.

Firestone, M., Firestone, B., and Tiedje, J. M.: Nitrous Oxide from Soil Denitrification: Factors Controlling Its Biological  
Production, Science, 208, 749-751, doi:10.1126/science.208.4445.749, 1980.



Grabb, K. C., Buchwald, C., Hansel, C. M., and Wankel, S. D.: A dual nitrite isotopic investigation of chemodenitrification by mineral-associated Fe(II) and its production of nitrous oxide, *Geochim. Cosmochim. Acta*, 196, 388-402, 395 <https://doi.org/10.1016/j.gca.2016.10.026>, 2017.

Hama-Aziz, Z. Q., Hiscock, K. M., and Cooper, R. J.: Dissolved nitrous oxide (N<sub>2</sub>O) dynamics in agricultural field drains and headwater streams in an intensive arable catchment, *Hydrological Processes*, 31, 1371-1381, <https://doi.org/10.1002/hyp.11111>, 2017.

Haynes, W.: Bonferroni Correction, in: *Encyclopedia of Systems Biology*, edited by: Dubitzky, W., Wolkenhauer, O., Cho, K.-H., and Yokota, H., Springer New York, New York, NY, 154-154, 10.1007/978-1-4419-9863-7\_1213, 2013.

Hinshaw, S. E. and Dahlgren, R. A.: Dissolved Nitrous Oxide Concentrations and Fluxes from the Eutrophic San Joaquin River, California, *Environmental Science & Technology*, 47, 1313-1322, 10.1021/es301373h, 2013.

IPCC: 2019 Refinement to the 2006 IPCC Guidelines for National Greenhouse Gas Inventories, Intergovernmental Panel on Climate Change, 2019.

Jurado, A., Borges, A. V., and Brouyère, S.: Dynamics and emissions of N<sub>2</sub>O in groundwater: A review, *Science of The Total Environment*, 584-585, 207-218, <https://doi.org/10.1016/j.scitotenv.2017.01.127>, 2017.

Knowles, R.: Denitrification, *Microbiological reviews*, 46, 43-70, 1982.

Kroeze, C., Bouwman, A., and Slomp, C. P.: Sinks for nitrous oxide at the earth's surface, *Greenhouse gas sinks*, 2007.

Lenth, R.: Estimated Marginal Means, aka Least-Squares Means (R package version 1.11.2), Retrieved from <https://CRAN.R-project.org/package=emmeans>, 2025.

Liu, B., Frostegård, Å., and Bakken, L. R.: Impaired Reduction of N<sub>2</sub>O to N<sub>2</sub> in Acid Soils Is Due to a Posttranscriptional Interference with the Expression of nosZ, *mBio*, 5, 10.1128/mbio.01383-01314, doi:10.1128/mbio.01383-14, 2014.

Maavara, T., Lauerwald, R., Laruelle, G. G., Akbarzadeh, Z., Bouskill, N. J., Van Cappellen, P., and Regnier, P.: Nitrous oxide emissions from inland waters: Are IPCC estimates too high?, *Global Change Biology*, 25, 473-488, 415 <https://doi.org/10.1111/gcb.14504>, 2019.

Madsen, H. B.: *Kompendium i jordbundsgeografi*, 1987.

Marzadri, A., Amatulli, G., Tonina, D., Bellin, A., Shen, L. Q., Allen, G. H., and Raymond, P. A.: Global riverine nitrous oxide emissions: The role of small streams and large rivers, *Science of The Total Environment*, 776, 145148, <https://doi.org/10.1016/j.scitotenv.2021.145148>, 2021.

Mulholland, P. J., Helton, A. M., Poole, G. C., Hall, R. O., Hamilton, S. K., Peterson, B. J., Tank, J. L., Ashkenas, L. R., Cooper, L. W., Dahm, C. N., Dodds, W. K., Findlay, S. E. G., Gregory, S. V., Grimm, N. B., Johnson, S. L., McDowell, W. H., Meyer, J. L., Valett, H. M., Webster, J. R., Arango, C. P., Beaulieu, J. J., Bernot, M. J., Burgin, A. J., Crenshaw, C. L., Johnson, L. T., Niederlehner, B. R., O'Brien, J. M., Potter, J. D., Sheibley, R. W., Sobota, D. J., and Thomas, S. M.: Stream denitrification across biomes and its response to anthropogenic nitrate loading, *Nature*, 452, 202-205, 10.1038/nature06686, 425 2008.



Mwanake, R. M., Gettel, G. M., Wangari, E. G., Butterbach-Bahl, K., and Kiese, R.: Interactive effects of catchment mean water residence time and agricultural area on water physico-chemical variables and GHG saturations in headwater streams, *Frontiers in Water*, Volume 5 - 2023, 10.3389/frwa.2023.1220544, 2023.

Olaya-Abril, A., Hidalgo-Carrillo, J., Luque-Almagro, V. M., Fuentes-Almagro, C., Urbano, F. J., Moreno-Vivián, C., 430 Richardson, D. J., and Roldán, M. D.: Effect of pH on the denitrification proteome of the soil bacterium *Paracoccus denitrificans* PD1222, *Scientific Reports*, 11, 17276, 10.1038/s41598-021-96559-2, 2021.

Peterse, I., Carstensen, M. V., Seelen, A.-M., Lücker, S., Audet, J., and Veraart, A. J.: Microbial N<sub>2</sub>O and CH<sub>4</sub> cycling in streams respond differently to land use and low pH, in prep.

Qiu, Y., Zhang, Y., Zhang, K., Xu, X., Zhao, Y., Bai, T., Zhao, Y., Wang, H., Sheng, X., Bloszies, S., Gillespie, C. J., He, T., 435 Wang, Y., Chen, H., Guo, L., Song, H., Ye, C., Wang, Y., Woodley, A., Guo, J., Cheng, L., Bai, Y., Zhu, Y., Hallin, S., Firestone, M. K., and Hu, S.: Intermediate soil acidification induces highest nitrous oxide emissions, *Nat Commun*, 15, 2695, 10.1038/s41467-024-46931-3, 2024.

Quick, A. M., Reeder, W. J., Farrell, T. B., Tonina, D., Feris, K. P., and Benner, S. G.: Nitrous oxide from streams and rivers: A review of primary biogeochemical pathways and environmental variables, *Earth-Science Reviews*, 191, 224-262, 440 <https://doi.org/10.1016/j.earscirev.2019.02.021>, 2019.

R Core Team: R: A language and environment for statistical computing [code], 2025.

Ravishankara, A. R., Daniel, J. S., and Portmann, R. W.: Nitrous oxide (N<sub>2</sub>O): the dominant ozone-depleting substance emitted in the 21st century, *Science*, 326, 123-125, 10.1126/science.1176985, 2009.

Reay, D. S., Smith, K. A., and Edwards, A. C.: Nitrous oxide emission from agricultural drainage waters, *Global Change Biology*, 9, 195-203, <https://doi.org/10.1046/j.1365-2486.2003.00584.x>, 2003.

Rosamond, M. S., Thuss, S. J., and Schiff, S. L.: Dependence of riverine nitrous oxide emissions on dissolved oxygen levels, *Nature Geoscience*, 5, 715-718, 10.1038/ngeo1556, 2012.

Seitzinger, S. P. and Kroeze, C.: Global distribution of nitrous oxide production and N inputs in freshwater and coastal marine ecosystems, *Global Biogeochemical Cycles*, 12, 93-113, <https://doi.org/10.1029/97GB03657>, 1998.

450 Silverthorn, T., Audet, J., Evans, C. D., van der Knaap, J., Kosten, S., Paranaíba, J., Struik, Q., Webb, J., Wu, W., Yan, Z., and Peacock, M.: The Importance of Ditches and Canals in Global Inland Water CO<sub>2</sub> and N<sub>2</sub>O Budgets, *Global Change Biology*, 31, e70079, <https://doi.org/10.1111/gcb.70079>, 2025.

Šimek, M. and Cooper, J. E.: The influence of soil pH on denitrification: progress towards the understanding of this interaction over the last 50 years, *European Journal of Soil Science*, 53, 345-354, <https://doi.org/10.1046/j.1365-2389.2002.00461.x>, 2002.

455 Stow, C. A., Walker, J. T., Cardoch, L., Spence, P., and Geron, C.: N<sub>2</sub>O Emissions from Streams in the Neuse River Watershed, North Carolina, *Environmental Science & Technology*, 39, 6999-7004, 10.1021/es0500355, 2005.

Thodsen, H., Kjær, C., Tornbjerg, H., Rolighed, J., Larsen, S. E., and Blicher-Mathiesen, G.: Vandløb 2022, Aarhus Universitet, DCE – Nationalt Center for Environment og Energy, 2024.



460 Tonina, D., Marzadri, A., Bellin, A., Dee, M. M., Bernal, S., and Tank, J. L.: Nitrous Oxide Emissions From Drying Streams  
and Rivers, *Geophysical Research Letters*, 48, e2021GL095305, <https://doi.org/10.1029/2021GL095305>, 2021.

465 von der Heide, C., Böttcher, J., Deurer, M., Weymann, D., Well, R., and Duijnisveld, W. H. M.: Spatial variability of N<sub>2</sub>O concentrations and of denitrification-related factors in the surficial groundwater of a catchment in Northern Germany, *Journal of Hydrology*, 360, 230-241, <https://doi.org/10.1016/j.jhydrol.2008.07.034>, 2008.

470 Wankel, S. D., Ziebis, W., Buchwald, C., Charoenpong, C., de Beer, D., Dentinger, J., Xu, Z., and Zengler, K.: Evidence for fungal and chemodenitrification based N<sub>2</sub>O flux from nitrogen impacted coastal sediments, *Nature Communications*, 8, 15595, 10.1038/ncomms15595, 2017.

475 Webb, J. R., Hayes, N. M., Simpson, G. L., Leavitt, P. R., Baulch, H. M., and Finlay, K.: Widespread nitrous oxide undersaturation in farm waterbodies creates an unexpected greenhouse gas sink, *Proceedings of the National Academy of Sciences*, 116, 9814-9819, doi:10.1073/pnas.1820389116, 2019.

480 Wrage, N., Velthof, G. L., van Beusichem, M. L., and Oenema, O.: Role of nitrifier denitrification in the production of nitrous oxide, *Soil Biology and Biochemistry*, 33, 1723-1732, [https://doi.org/10.1016/S0038-0717\(01\)00096-7](https://doi.org/10.1016/S0038-0717(01)00096-7), 2001.

485 Yao, Y., Tian, H., Shi, H., Pan, S., Xu, R., Pan, N., and Canadell, J. G.: Increased global nitrous oxide emissions from streams and rivers in the Anthropocene, *Nature Climate Change*, 10, 138-142, 10.1038/s41558-019-0665-8, 2020.

Zhu-Barker, X., Cavazos, A. R., Ostrom, N. E., Horwath, W. R., and Glass, J. B.: The importance of abiotic reactions for 490 nitrous oxide production, *Biogeochemistry*, 126, 251-267, 10.1007/s10533-015-0166-4, 2015.

Zuur, A. F., Leno, E. N., Walker, N., Savelie, A. A., and Smith, G. M.: *Mixed Effects Models and Extensions in Ecology with R., Statistics for Biology and Health*, Springer New York, NY, XXII, 574 pp., <https://doi.org/10.1007/978-0-387-87458-6>, 2009.

480

485



490

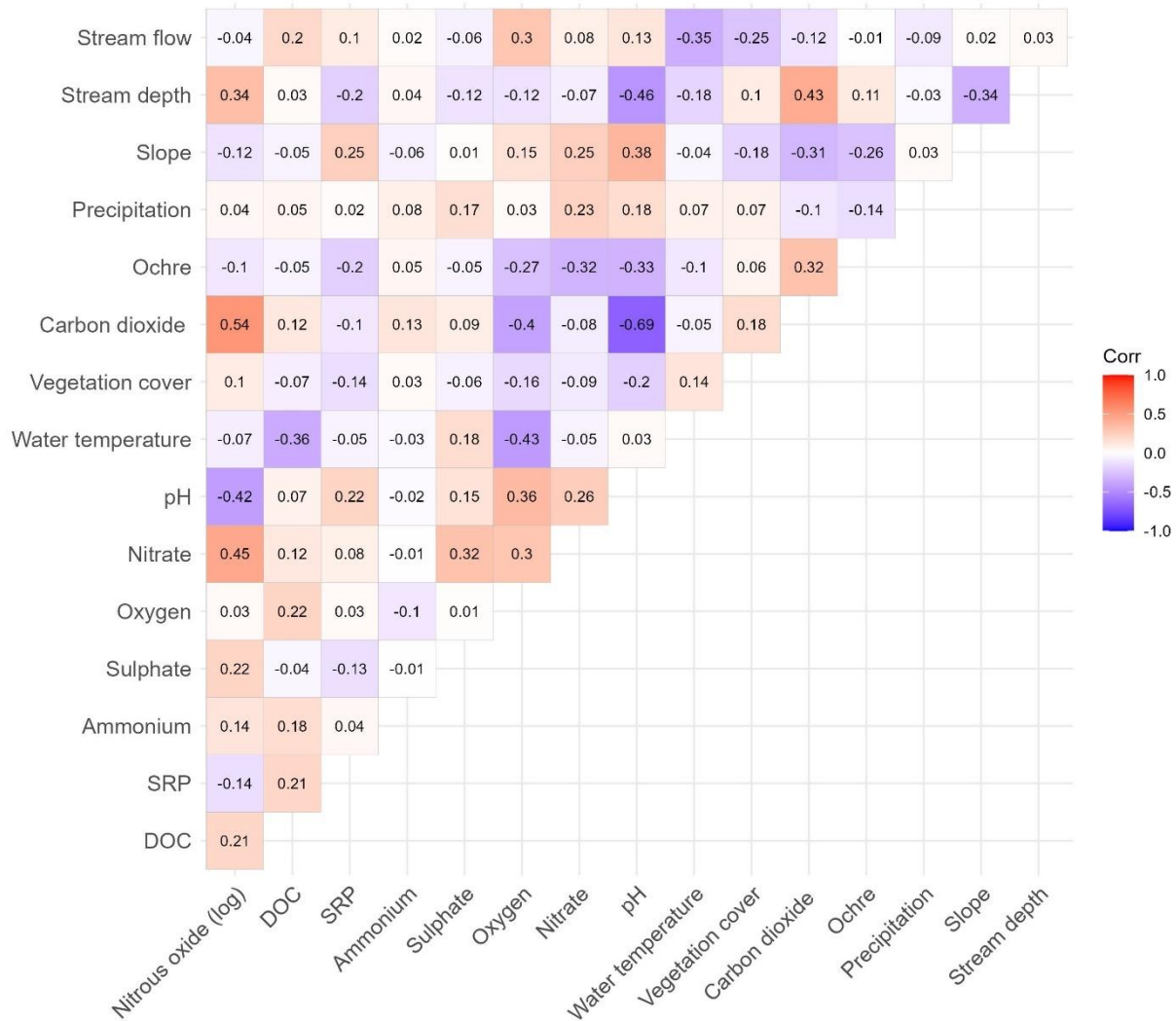
## Appendix A

### 2. Methods

#### 2.5 Sediment analysis

Dry matter content was determined following Ds/En 15934 (2012). Approximately 5 g of homogenized soil was weighed into 495 pre-weighed ceramic crucibles and dried at 105°C for 70 hours. Samples were weighed in triplicate per site. After drying, samples were transferred to a desiccator and stored until further analysis. The desiccator remained open for 20 minutes post-drying to prevent condensation. The loss on ignition, following Ds/En 15934 (2012), was determined by annealing the dry matter at  $550\text{ }^{\circ}\text{C} \pm 25\text{ }^{\circ}\text{C}$  for at least 2 hours in a muffle furnace. The crucibles were then cooled briefly on a metal plate, followed by cooling in a desiccator. The desiccator lid remained open for at least one hour post-transfer to avoid condensation. 500 Once samples reached room temperature, they were weighed to determine organic matter content. The carbon-to-nitrogen (C:N) ratio of stream sediment samples was determined using a Thermo Scientific™ FlashSmart™ Elemental Analyzer. Approximately 25–30 mg of oven-dried sediment was sealed in tin capsules and combusted at 950°C in a quartz reactor packed with quartz wool, copper oxide, and electrolytic copper. Nitrogen and carbon were subsequently separated chromatographically and detected via thermal conductivity.

505



510

**Figure A1. Correlation plots based on Pearson's correlation coefficients, where unit of nitrous oxide is percentage saturation, stream flow is  $\text{m s}^{-1}$ , stream depth is cm, slope is permille, precipitation is mm, ochre is on scale from 0-3, vegetation cover in percentage, water temperature in Celsius degrees, carbon dioxide is  $\text{ug L}^{-1}$ , and units of nitrate, oxygen, sulphate, ammonium, SRP (soluble reactive phosphorus) and DOC (dissolved organic carbon) are  $\text{mg L}^{-1}$ .**

515

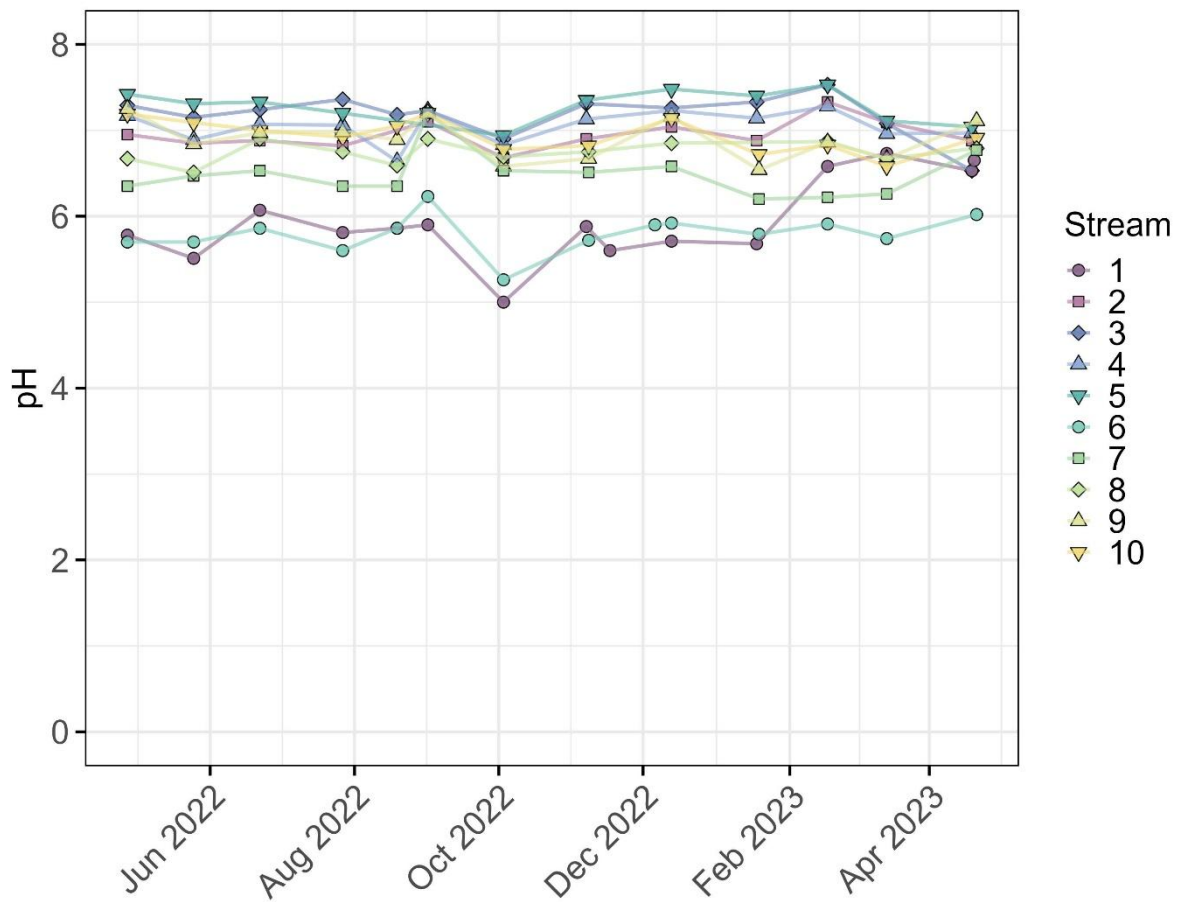
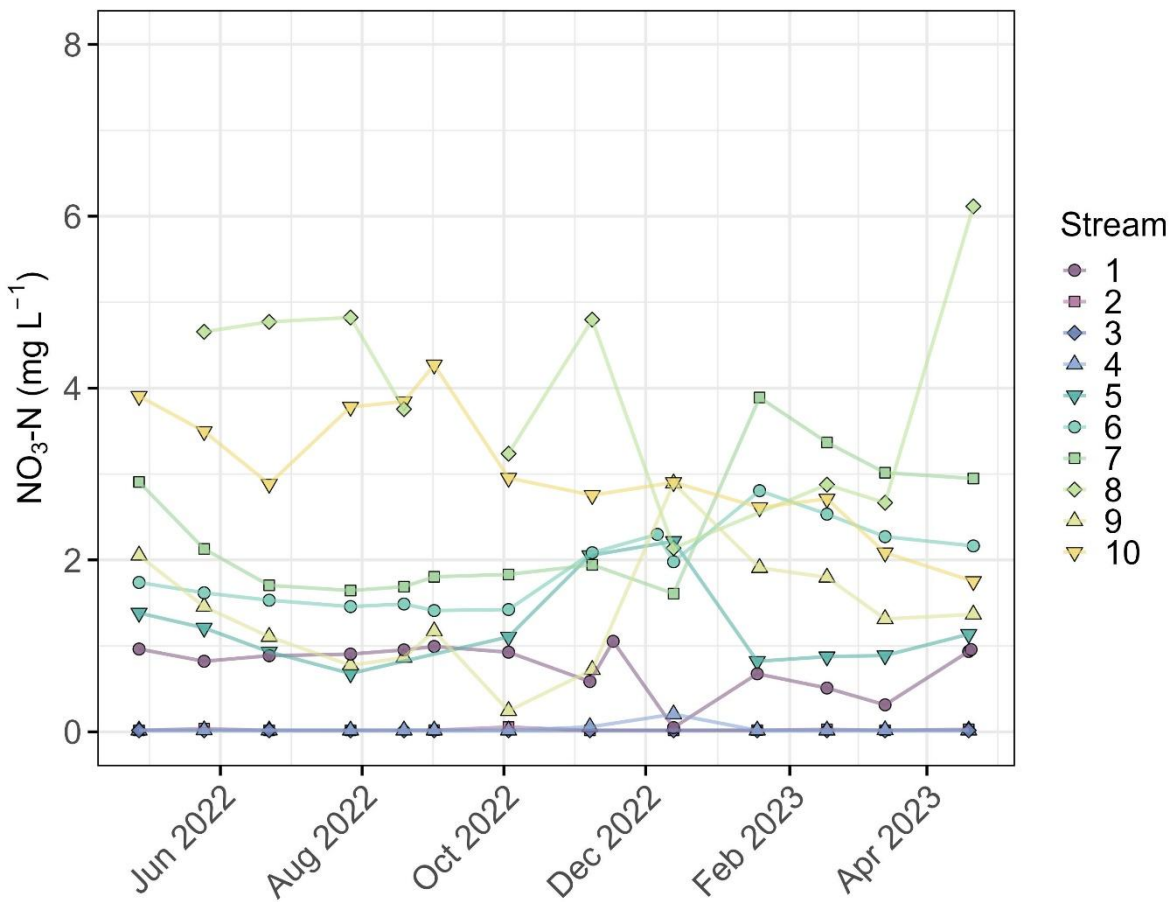


Figure A2. The pH measured in the water column from the ten streams (1-10) with monthly monitoring.



520 Figure A3. The nitrate ( $\text{NO}_3^-$ ) concentration of water from the ten streams (1-10) with monthly monitoring.

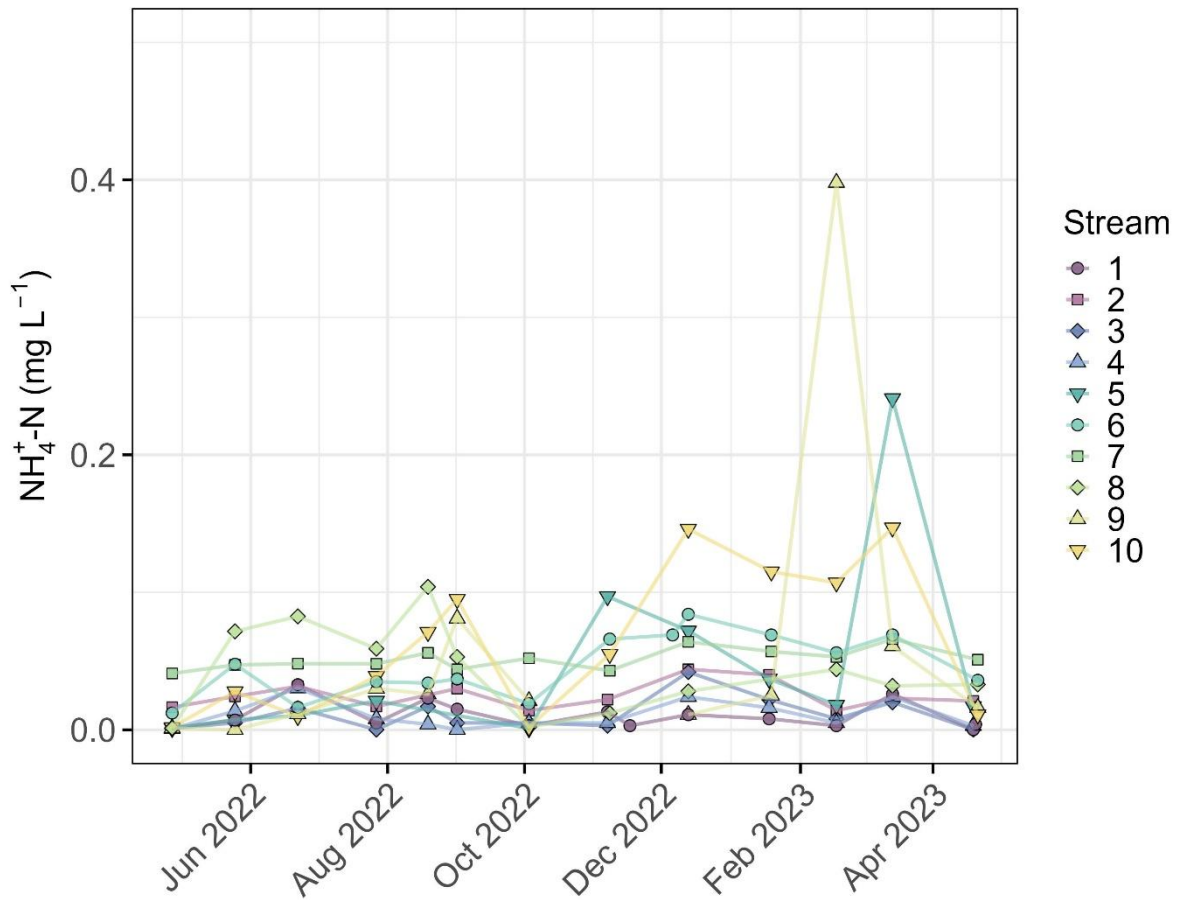
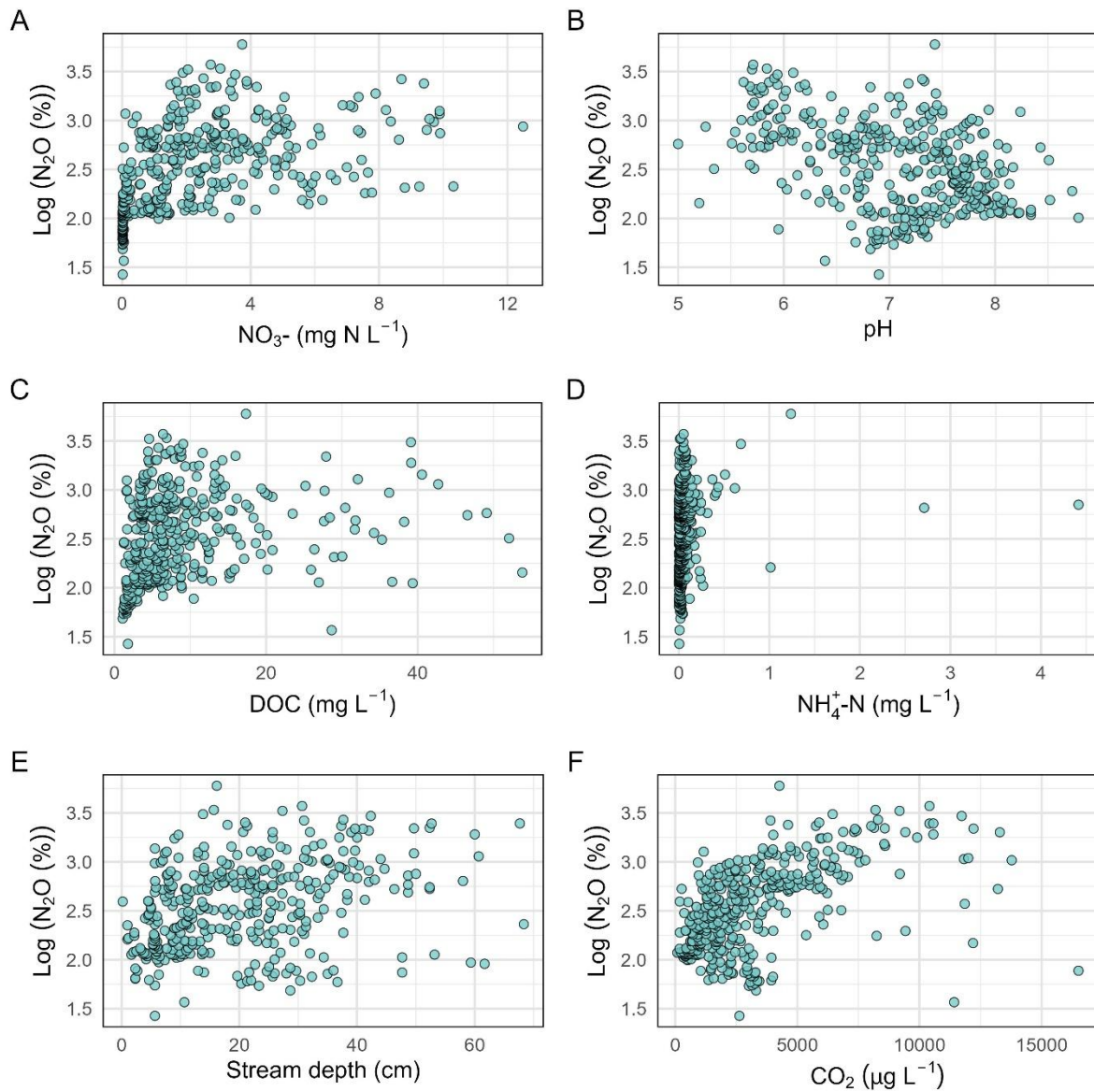
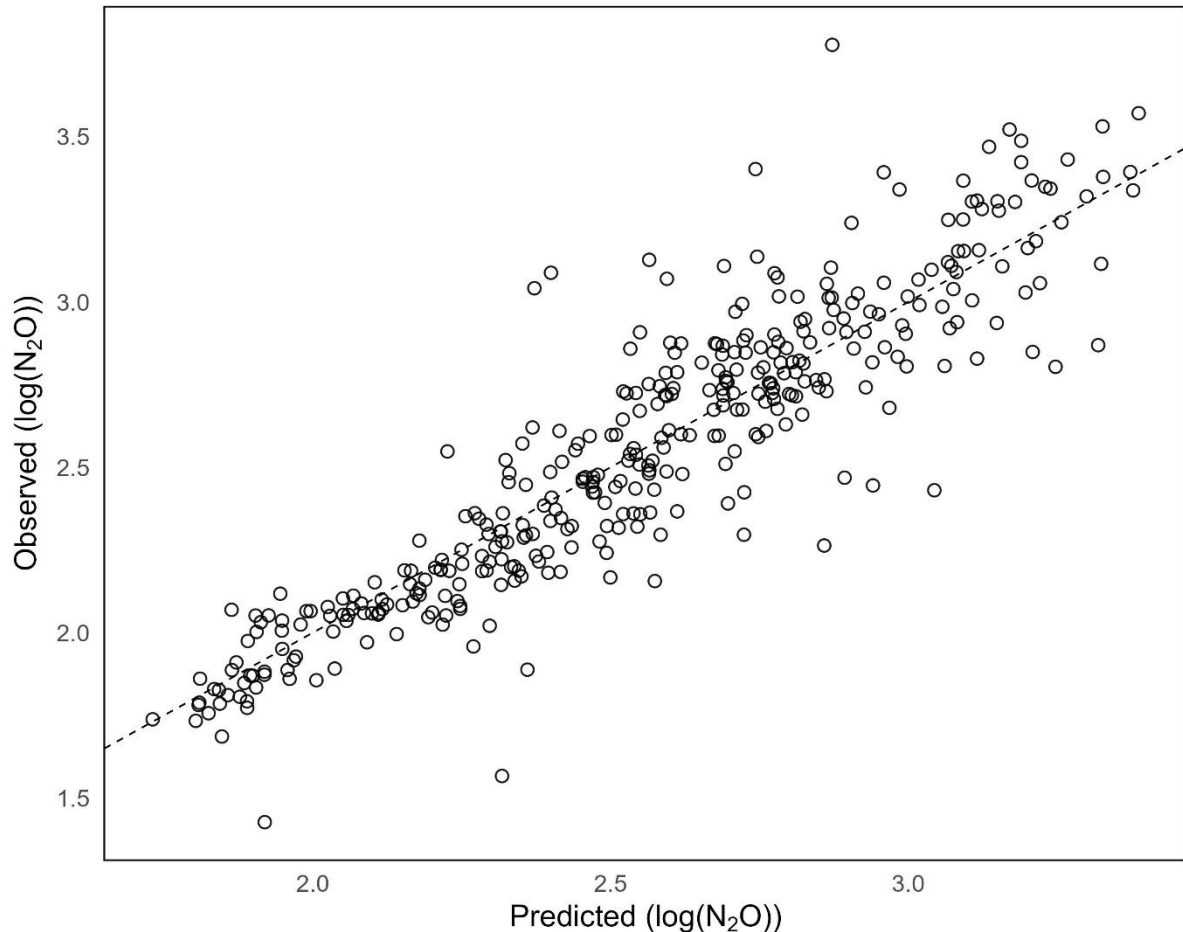


Figure A4. The ammonium ( $\text{NH}_4^+$ ) concentration of water from the ten streams (1-10) with monthly monitoring. A  $\text{NH}_4^+$  concentration of  $4.4 \text{ mg L}^{-1}$  from stream 9 from the 8 November 2022 was omitted from the graph for visual reasons.



**Figure A5. Stream water nitrous oxide (N<sub>2</sub>O) saturation plotted against nitrate (NO<sub>3</sub><sup>-</sup>) (A), pH (B), dissolved organic carbon (DOC) (C), ammonium (NH<sub>4</sub><sup>+</sup>) (D), and stream depth (E) for Danish headwater streams.**



530

**Figure A6.** Predicted versus observed values of stream water nitrous oxide (N<sub>2</sub>O) saturation.

535

540

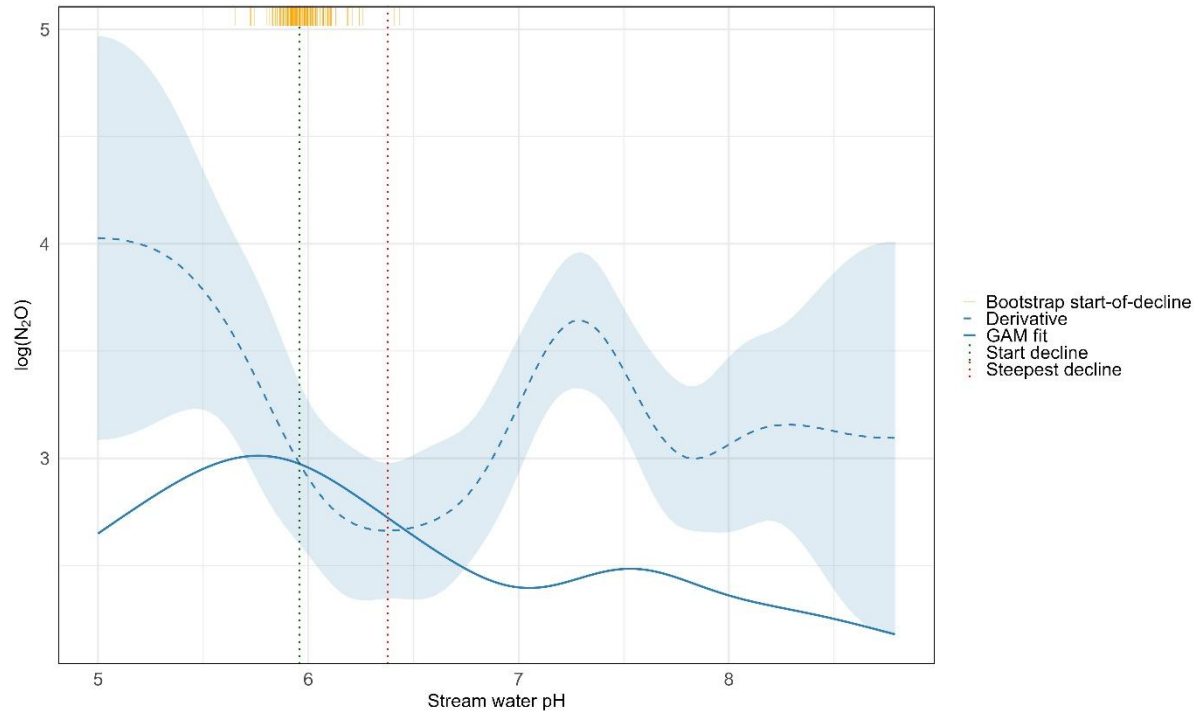


**Figure A7. Generalized additive model (GAM) of  $\log(\text{N}_2\text{O})$  saturation vs. stream water pH. Solid blue line: predicted  $\log(\text{N}_2\text{O})$ ; dashed blue line: derivative with 95 % confidence interval (shaded). Vertical dotted lines: start of decline (green) and steepest decline (red). Orange rug: bootstrap distribution of start-of-decline pH values.**

545

550

555



560

**Table A1.** Variance inflation factor (VIF) analysis of linear mixed-effects model (parameters included: nitrate, pH, stream depth, land use and interaction nitrate\*pH). All continuous predictor variables were standardized (z-transformed: centered and scaled to unit variance), stream water during summer 2022, autumn 2022, winter 2022 and spring 2023, where N<sub>2</sub>O =nitrous oxide, NO<sub>3</sub><sup>-</sup>=nitrate, NH<sub>4</sub><sup>+</sup> =ammonium, and DOC =dissolved organic carbon.

Variable	VIF
NO <sub>3</sub> <sup>-</sup> _z	1.3
pH_z	1.2
DOC_z	1.1
NH <sub>4</sub> <sup>+</sup> _z	1.0
Depth_z	1.2
NO <sub>3</sub> <sup>-</sup> _z:pH_z	1.3

565

**Table A2.** Characteristics of stream water during summer 2022, autumn 2022, winter 2022 and spring 2023, where N<sub>2</sub>O =nitrous oxide, NO<sub>3</sub><sup>-</sup>=nitrate, TN= total nitrogen, NH<sub>4</sub><sup>+</sup> =ammonium, CO<sub>2</sub>= carbon dioxide, TOC =total organic carbon, DOC =dissolved organic carbon, TP=total phosphorus, SRP =soluble reactive phosphorus, SO<sub>4</sub><sup>2-</sup>=sulphate, and O<sub>2</sub>= dissolved oxygen.

	Winter	Spring	Summer	Autumn 570
<b>Sample size</b>	93	110	85	90
<b>Precipitation (mm)</b>	243 (48)	145 (21)	153 (28)	200 (25)
<b>Temperature (water)</b>	4.7 (1.6)	9.4 (2.0)	13.3 (2.2)	10.0 (1.4)
<b>Flow velocity (m s<sup>-1</sup>)</b>	0.34 (0.23)	0.27 (0.20)	0.13 (0.15)	0.19 (0.20)
N <sub>2</sub> O sat (%)	710 (766)	570 (658)	431 (415)	632 (800)
N <sub>2</sub> O (µg L <sup>-1</sup> )	3.1 (3.3)	2.1 (2.4)	1.4 (1.4)	2.5 (3.0)
TN (mg L <sup>-1</sup> )	3.5 (2.4)	3.1 (2.4)	2.6 (2.8)	3.2 (3.7)
NO <sub>3</sub> <sup>-</sup> (mg L <sup>-1</sup> )	2.7 (2.1)	2.5 (2.3)	2.2 (2.7)	2.6 (2.5)
NH <sub>4</sub> <sup>+</sup> (mg L <sup>-1</sup> )	0.11 (0.29)	0.04 (0.07)	0.05 (0.12)	0.11 (0.48)
CO <sub>2</sub> (µg L <sup>-1</sup> )	2042 (1759)	2036 (1794)	2227 (1990)	2899 (2319)
TOC (mg L <sup>-1</sup> )	16.6 (13.7)	9.2 (7.8)	5.4 (3.1)	9.5 (7.0)
DOC (mg L <sup>-1</sup> )	14.7 (12.9)	8.4 (7.4)	4.7 (2.7)	8.2 (6.3)
TP (mg L <sup>-1</sup> )	0.20 (0.49)	0.16 (0.42)	0.44 (3.10)	0.33 (1.02)
SRP (mg L <sup>-1</sup> )	0.05 (0.04)	0.03 (0.02)	0.05 (0.03)	0.09 (0.08)
SO <sub>4</sub> <sup>2-</sup> (mg L <sup>-1</sup> )	25.1 (14.7)	24.2 (14.0)	32.1 (20.2)	30.6 (19.1)
O <sub>2</sub> (mg L <sup>-1</sup> )	10.9 (2.3)	10.7 (2.3)	8.1 (2.3)	8.2 (2.5)
pH	7.0 (0.7)	7.1 (0.8)	7.1 (0.7)	7.0 (0.7)
<b>Stream depth (cm)</b>	25 (14)	20 (13)	16 (14)	21 (12)



585

**Table A3. Results from linear mixed-effects model analysis with pairwise test of seasonal difference in N2O saturation (%).**

	<b>Estimate</b>	<b>SE</b>	<b>df</b>	<b>t ratio</b>	<b>p value</b>
<b>Autumn - Spring</b>	0.04	0.03	303	1.3	0.57
<b>Autumn - Summer</b>	0.15	0.04	304	4.1	<0.001
<b>Autumn - Winter</b>	-0.04	0.03	304	-1.0	0.73
<b>Spring - Summer</b>	0.11	0.03	304	3.1	<0.05
<b>Spring - Winter</b>	-0.08	0.03	303	-2.4	0.08
<b>Summer - Winter</b>	-0.18	0.04	305	-5.2	<0.001

590

**Table A4. Model performance of linear mixed-effects model (parameters included: nitrate, pH, ammonium, stream depth, land use and interaction nitrate\*pH). All continuous predictor variables were standardized (z-transformed: centered and scaled to unit variance).**

<b>Model</b>	<b>AIC</b>	<b>AIC</b>	<b>AICc</b>	<b>AICc</b>	<b>BIC</b>	<b>BIC</b>	<b>R2</b>	<b>R2</b>	<b>ICC</b>	<b>RMSE</b>		
			<b>weight</b>		<b>weight</b>		<b>weight</b>	<b>(cond.)</b>	<b>(marg.)</b>			
	1.6	<.001		2.1	<.001		36.9	<.001	0.734	0.465	0.503	0.185

600 **References**

DS/EN 15934, 2012. Sludge, treated biowaste, soil and waste – Calculation of dry matter fraction after determination of dry residue or water content, in: standard, D. (Ed.).